Bioorganic & Medicinal Chemistry Letters 20 (2010) 3142–3145

Contents lists available at ScienceDirect

Bioorganic & Medicinal Chemistry Letters

journal homepage: www.elsevier.com/locate/bmcl

# Exploration of the HDAC2 foot pocket: Synthesis and SAR of substituted *N*-(2-aminophenyl)benzamides

Jerome C. Bressi, Andy J. Jennings, Robert Skene, Yiqin Wu, Robert Melkus, Ron De Jong, Shawn O'Connell, Charles E. Grimshaw, Marc Navre, Anthony R. Gangloff *

*Takeda San Diego, 10410 Science Center Drive, San Diego, CA 92121, USA*

ARTICLE INFO

*Article history:*
Received 29 January 2010
Revised 25 March 2010
Accepted 26 March 2010
Available online 30 March 2010

*Keywords:*
Histone deacetylase inhibitors
HDAC
Oncology

ABSTRACT

A series of *N*-(2-amino-5-substituted phenyl)benzamides (**3**–**21**) were designed, synthesized and evaluated for their inhibition of HDAC2 and their cytotoxicity in HCT116 cancer cells. Multiple compounds from this series demonstrated time-dependent binding kinetics that is rationalized using a co-complex crystal structure of HDAC2 and *N*-(4-aminobiphenyl-3-yl)benzamide (**6**).



The balance of reversible acetylation and deacetylation of histones is critical to the regulation of chromatin structure, and it directly affects gene expression in eukaryotic organisms. Histone deacetylases (HDACs), a class of Zn metalloenzymes, catalyze the deacetylation of lysine residues in histones and facilitate the structural stabilization of nucleosomes necessary for the first level of DNA organization.[1,2] Histone acetyltransferase (HAT) maintains the balance of deacetylation.[3,4] Perturbations of this balance have been linked to cancer and inhibition of HDACs results in the expression of genes that produce terminal differentiation, growth arrest and/or apoptosis in a variety of cancer cells.[1,5] Inhibition of HDACs has been identified as a mechanism for treating cancer, and multiple small-molecule HDAC inhibitors are advancing in clinical trials.[6–9] In addition, HDAC inhibitors have proven useful in the treatment or prevention of protozoal diseases[10] and psoriasis.[11]

Published small-molecule HDAC inhibitors typically contain a bidentate chelator, or warhead, that interacts with the catalytic $Zn^{2+}$ that is nestled 8 Å deep in the protein active site. The two most common chelators found in these molecules are hydroxamates and anilidesas exemplified by SAHA[12] and MS-275,[9] respectively (Fig. 1). Previously published crystal structures of HDLP[13] (an HDAC homolog) and HDAC8[14] demonstrate how hydroxamate inhibitors are coordinated to the catalytic zinc as the tether sits in a hydrophobic tunnel capped with a moiety that sits at the solvent protein interface. However, a 14 Å long internal cavity or 'foot pocket' adjacent to the catalytic zinc remains unoccupied. While others have suggested inhibitors which could make use of the foot pocket through modeling,[15,16] no crystallographic evidence has been presented in HDAC8 or HDLP which shows specific examples accessing the foot pocket.

Analysis of HDAC2 crystal co-complexes[17] obtained in our laboratories with both hydroxamates and anilides revealed that the anilides accessed the foot pocket adjacent to the zinc binding site that, by its nature of atom connectivity, the hydroxamate could not. To explore this binding region more thoroughly, we used *N*-(2-aminophenyl)benzamide as the minimal scaffold required to interact with the HDAC2 catalytic machinery. Inspection of the HDAC2 crystal structure suggested that substitutions off of the 5-position of *N*-(2-aminophenyl)benzamides would provide the appropriate vector for reaching towards interactions with the foot pocket. We designed and synthesized a series of *N*-(2-amino-5-substituted phenyl)benzamides (**3–21**) and evaluated them in an HDAC2 enzyme assay and cellular assays.

The synthesis of *N*-(2-amino-5-substituted phenyl)benzamides (Scheme 1) begins with Boc protection of the commercially available 4-bromo-2-nitroaniline (**1**). Reduction of the nitro group and subsequent acylation with benzoylchloride provides *tert*-butyl 2-benzamido-4-bromophenylcarbamate (**2**). Standard Suzuki coupling conditions followed by removal of the Boc group provided the desired compounds (**4–21**). Substituting with the appropriate starting material, compound **3** was synthesized using standard methodology.[18]

Benzamides were evaluated as inhibitors of recombinant human HDAC2 using a protease coupled end-point assay with Ac-Lys(Ac)-AMC as a substrate. The reaction product was quantified by

* Corresponding author. Tel.: +1 858 731 3531; fax: +1 858 550 0526.
*E-mail address:* agangloff@takedasd.com (A.R. Gangloff).

0960-894X/$ - see front matter © 2010 Elsevier Ltd. All rights reserved.
doi:10.1016/j.bmcl.2010.03.091

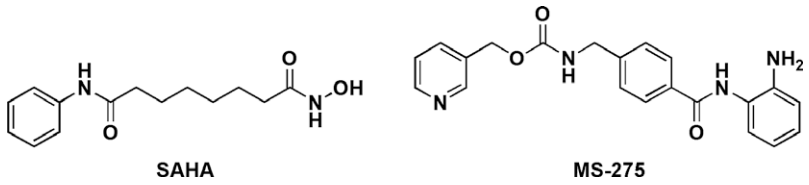


**Figure 1.** SAHA (hydroxamate chelator) and MS-275 (anilide chelator).

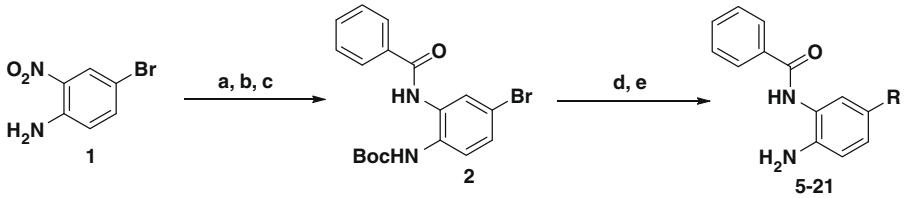


**Scheme 1.** Reagents and conditions: (a) $Boc_2O$, $Et_3N$, DMF, rt, 16 h; (b) EtOH/AcOH, Zn (dust), reflux, 30 min; (c) PhC(O)Cl, $Et_3N$, DMF, rt, 2 h; (d) R–$B(OH)_2$, $(Ph_3P)_4Pd$, 2 M $Na_2CO_3$, dioxane, reflux, 18 h; (e) DCM/TFA, rt, 1 h.

fluorescence at 480 nm with excitation wavelength at 370 nm. The activity of the benzamides was evaluated separately after 1 h and 24 h pre-incubation of inhibitor with HDAC2 (Table 1). Most of the benzamides inhibited HDAC2 in the $pIC_{50}$ range of 4.6–6.1 without pre-incubation. There was, however, a notable time-dependent inhibition upon pre-incubation of inhibitor with HDAC2 at 24 h resulting in increased inhibition for most compounds. Indeed, compounds **5**, **8**, **12**, **18** and **20** demonstrated a 21–42-fold increase in enzymatic inhibition. Compounds with large R groups, such as benzothiophenes **7** and **15**, along with benzofuran **19** did not display any difference in enzymatic potency between the two assays. In contrast, no time-dependence was noted with hydroxamate inhibitors such as SAHA.

Compounds were also evaluated for cytotoxicity in a human HCT116 colon cancer cell line. $EC_{50}$ determinations were calculated from remaining cell viability after 72 h incubation using the MTS calorimetric readout (Table 1). In general, compounds with enzymatic activity below 100 nM in the 24 h pre-incubation assay exhibited some level of cellular activity. Compounds **5** and **8** demonstrated $EC_{50}$s of 1.1 and 2.1 μM, respectively.

**Table 1**
Enzymatic and cellular activity of substituted *N*-(2-aminophenyl)benzamides

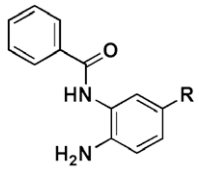


| Compd | R | HDAC2 inhibition 1 h-$IC_{50}$[b] | HDAC2 inhibition 24 h-$IC_{50}$[c] | Δ | Cytotoxicity HCT116 $EC_{50}$[a] |
|---|---|---|---|---|---|
| **3** | H | 10 | 3.1 | 3× | na |
| **4** | 2-Thiazolyl | 5.8 | 0.39 | 14× | 31 |
| **5** | Phenyl | 0.90 | 0.027 | 33× | 1.1 |
| **6** | 4-Vinylphenyl | 5.0 | 0.80 | 6× | na |
| **7** | 2-Benzothiophenyl | 10 | 10 | — | na |
| **8** | 3-Furanyl | 0.81 | 0.039 | 21× | 2.1 |
| **9** | 4-Pyridyl | 3.9 | 0.27 | 14× | 16 |
| **10** | 4-Methoxyphenyl | 0.86 | 0.14 | 6× | >20 |
| **11** | 4-Acetylphenyl | 5.0 | 3.8 | 1.3× | na |
| **12** | 2-Furanyl | 1.8 | 0.043 | 42× | 3.2 |
| **13** | 3-Methylphenyl | 7.2 | 3.1 | 2× | na |
| **14** | 3-Nitrophenyl | 200 | 21 | 10× | na |
| **15** | 3-Benzothiophenyl | 10 | 10 | — | na |
| **16** | 3-Acetylphenyl | 27 | 13 | 2 | na |
| **17** | 3-Methoxyphenyl | 3.4 | 1.3 | 2× | na |
| **18** | 4-Bromophenyl | 24 | 0.60 | 40× | >20 |
| **19** | 2-Benzofuranyl | 10 | 10 | — | na |
| **20** | 4-Fluorophenyl | 1.4 | 0.032 | 42× | 3.1 |
| **21** | 4-Trifluoromethyl-phenyl | 40 | 3.8 | 10 | na |
| SAHA | — | 0.076 | 0.072 | — | 2.0 |

[a] Values in μM are means of three experiments; na = not active.
[b] 1 h-$IC_{50}$ = 1 h reaction of benzamides with HDAC2 and substrate. Values in μM are means of three experiments.
[c] 24 h-$IC_{50}$ = 24 h incubation of benzamides with HDAC2 followed by 1 h reaction with substrate. Values in μM are means of three experiments.

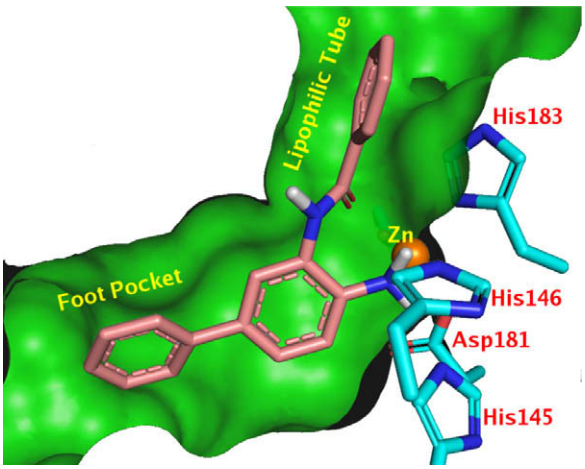


**Figure 2.** The X-ray crystal co-complex of compound **5** with HDAC2 showing the catalytic residues, the zinc atom (orange) and the surface of the site in green.

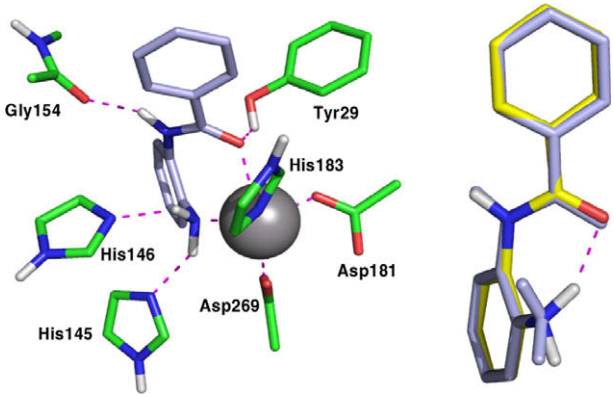


**Figure 3.** (Left) The system investigated by semi-empirical methods. The truncated anilide ligand is shown in light blue, the zinc as a silver sphere and the protein carbon atoms in green. Polar interactions are indicated by the dashed, magenta, lines. (Right) A comparison of the bound ligand conformation, with hydrogen atoms optimized with AM1, and the unbound ligand, fully-optimized at the 6-31G* level. The bound ligand conformation is shown in light blue. The carbon atoms of the unbound ligand are yellow with the internal hydrogen bond indicated by the dashed, magenta, line.

The HDAC2 active site consists of the catalytic machinery, a lipophilic 'tube' which leads from the surface to this machinery, and a 'foot pocket' immediately adjacent to the machinery. A zinc atom is held by Asp181, His183, and Asp269. The lipophilic tube is formed by Gly154, Phe155, His183, Phe210, and Leu276. The foot pocket residues are Tyr29, Met35, Phe114, and Leu144. This pocket contains multiple water molecules in co-complexes which lack a sizeable R group. Figure 2 shows the HDAC2 active site with **5** bound and illustrates the foot pocket occupied by the phenyl R group of **5**.

In order to study the mechanism behind the time-dependence observed, as well as suggest additional molecules for synthesis, a 1.46 Å co-complex structure was used as the basis for some semi-empirical calculations. Figure 3 shows the system simulated at the AM1 level with the program VAMP (version 8.0b; Clark, T. et al., Erlangen). For this work, only the hydrogen atoms were optimized due to the use of truncation and the availability of such high-resolution structural data. The figure shows the final geometry achieved and indicates the numerous polar interactions formed. It is interesting to note how the anilide nitrogen is a surrogate for the water molecule required during the hydrolysis of acetylated lysine residues in the natural processing by this enzyme. The interactions shown indicate why, in general, so few warheads with appreciable binding are known (many weaker warheads rely upon additional interactions around the surface of the protein and the top of the binding pocket).

To investigate the transition from the unbound solvated ligand to the bound form, a simulation was carried out at the 6-31G* level of theory using the package GAMESS-US.[19] The unbound ligand was also simulated with AM1/VAMP as for the full system and the resulting conformation agreed very well with that found at the 6-31G* level. Figure 3 shows the comparison between the bound (AM1) and unbound (6-31G*/AM1) conformations of the prototypical ligand used for this work. Of note are the positions of the hydrogen atoms. In the bound form, the hydrogen atoms of the *ortho*-$NH_2$ group are involved in hydrogen bonds with the side-chains of histidines 145 and 146, the nitrogen of the *ortho*-$NH_2$ group chelates the zinc, and the carbonyl oxygen interacts with both the tyrosine sidechain hydroxyl and the zinc. In the unbound conformation, the *ortho*-$NH_2$ group forms an internal hydrogen bond with the carbonyl oxygen. It is clear that the number of complimentary interactions formed upon binding to the HDAC active site outweigh the dual penalties of ligand desolvation (approx 4.4 kcal/mol for the unbound conformation using the AM1/SCRF method in VAMP) and the disruption of the internal hydrogen bond. It is the latter which seems likely to be responsible for the time-dependence observed. The gross conformation of the anilides does not appear to change by a great deal upon binding to the HDAC active site and this binding can occur with the internal hydrogen bond intact (though the ligand will not be able to access the pocket as deeply). However, a proportion of these transiently-bound molecules will experience the hydrogen translation described in Figure 3 and form a substantially more stable complex with the active site. By Le Chatelier's principle, over time these transiently-bound forms will be converted to the tightly-bound, pseudo-irreversible form until an equilibrium is reached. This equilibrium is responsible for the final $IC_{50}$ observed for this class.

Using compound **3** as a reference compound, one can go further to explain the variable time-dependence with the choice of R group. As the size of R increases, the more difficult it will be for compounds to access the active site and undergo the described hydrogen bond translation. However, once bound, the reverse process will also be relatively slow. Of course, a point is reached at which the R group size is simply too large to allow acceptable access to the site and the affinities will be reduced as a result, at least over the time-frames considered here (e.g., compounds **7** and **15**). Figure 2 illustrates how these larger molecules will be at a disadvantage when accessing the active site deeply due to the bend in the tube from the surface to the foot pocket.

In conclusion, a series of simple benzamides were designed and synthesized to explore the 'foot pocket' area of the $Zn^{2+}$ active site of HDAC2. Some of these compounds inhibited the enzyme in the low micromolar range and exhibited moderate micromolar cellular potency in an HCT116 cancer cell line. Additionally, some of these benzamides demonstrated a time-dependent binding event that resulted in enzyme inhibition in the low nanomolar range after a 24-h incubation period with HDAC2. This time-dependent binging phenomena may positively affect the in vivo potency of anilides and merits further investigation.

## Acknowledgements

The authors would like to acknowledge Michael Organ and Debasis Mallik from Total Synthesis for synthetic support and Lu Zheng for analytical chemistry support.

## References and notes

1. Kousarides, T.; Verdel, A.; Lemercier, C.; Seigneurin-Berny, D. *Curr. Opin. Genet. Dev.* **1999**, *9*, 40.

2. Strahl, B. D.; Allis, C. D. *Nature* **2000**, *403*, 41.
3. Eberharter, A.; Becker, P. B. *EMBO Rep.* **2002**, *3*, 224.
4. Grozinger, C. M.; Schreiber, S. L. *Chem. Biol.* **2002**, *9*, 3.
5. Smith, K. T.; Workman, J. L. *Int. J. Biochem. Cell Biol.* **2008**, *41*, 21.
6. (a) Marks, P. A.; Richon, V. M.; Breslow, R.; Rifkind, R. A. *Curr. Opin. Oncol.* **2001**, *6*, 477–483; (b) Marks, P.; Rifkind, R. A.; Richon, V. M.; Breslow, R.; Miller, T.; Kelly, W. K. *Nat. Rev. Cancer* **2001**, *3*, 194; (c) Paris, M.; Porcelloni, M.; Binaschi, M.; Fattori, D. *J. Med. Chem.* **2008**, *51*, 3330.
7. Meinke, P. T.; Liberator, P. *Curr. Med. Chem.* **2000**, *8*, 211.
8. Remiszeweski, S. W.; Sambucetti, L. C.; Atadja, P.; Baiir, K. W.; Cornell, W. D.; Green, M. A.; Howell, K. L.; Jung, M.; Kown, P.; Trogani, N.; Walker, H. *J. Med. Chem.* **2002**, *45*, 753.
9. (a) Saito, A.; Yamashita, T.; Mariko, Y.; Nosaka, Y.; Nakanishi, O. *Proc. Natl. Acad. Sci. U.S.A.* **1999**, *96*, 4592; (b) Suzuki, T.; Ando, T.; Tsuchiya, K.; Fukazawa, N.; Saito, A.; Mariko, Y.; Yamashita, T.; Nakanishi, O. *J. Med. Chem.* **1999**, *42*, 3001.
10. Mai, A.; Cerbara, I.; Valente, S.; Massa, S.; Walker, L. A.; Tekwani, B. L. *Antimicrob. Agents Chemother.* **2004**, *48*, 1435.
11. McLaughlin, F.; La Thangue, N. B. *Curr. Drug Targets Inflamm. Allergy* **2004**, *3*, 213.
12. (a) Butler, L. M.; Agus, D. B.; Scher, H. I.; Higgins, B.; Rose, A.; Cordon-Cardo, C.; Thaler, H. T.; Rifkind, R. A.; Marks, P. A.; Richon, V. M. *Cancer Res.* **2000**, *60*, 5165; (b) Madeleine, D.; Jenny, V. *Expert Opin. Investig. Drugs* **2007**, *16*, 1111–1120; (c) Richon, V. M.; Garcia-Vargas, J.; Hardwick, J. S. *Cancer Lett.* **2009**, *280*, 201.
13. Finnin, M. S.; Donigian, J. R.; Cohen, A.; Richon, V. M.; Rifkind, R. A.; Marks, P. A.; Breslow, R.; Pavletich, N. P. *Nature* **1999**, *401*, 188.
14. (a) Somoza, J. R.; Skene, R. J.; Katz, B. A.; Mol, C.; Ho, J. D.; Jennings, A. J.; Luong, C.; Arvai, A.; Buggy, J. J.; Chi, E.; Tang, J.; Sang, B.-C.; Verner, E.; Wynands, R.; Leahy, E. M.; Dougan, D. R.; Snell, G.; Navre, M.; Knuth, M. W.; Swanson, R. V.; Mcree, D. E.; Tari, L. W. *Structure* **2004**, *12*, 1325; (b) Vannini, A.; Volpari, C.; Filocamo, G.; Caroli Casavola, E.; Brunetti, M.; Renzoni, D.; Chakravarty, P.; Paolini, C.; De Francesco, R.; Gallinari, P.; Steinckuhler, C.; Di Marco, S. *Proc. Nat. Acad. Sci. U.S.A.* **2004**, *101*, 15064.
15. (a) Wang, D.-F.; Wiest, O.; Helquist, P.; Lan-Hargest, H.-Y.; Wiech, N. L. *J. Med. Chem.* **2004**, *47*, 3409–3417; (b) Wang, D.-F.; Helquist, P.; Wiech, N. L.; Wiest, O. *J. Med. Chem.* **2005**, *48*, 6936; (c) Bieliaskas, A. V.; Pflum, M. K. H. *Chem. Soc. Rev.* **2008**, *37*, 1402; (d) Moradei, O. M.; Mallais, T. C.; Frechette, S.; Paquin, I.; Tessier, P. E.; Leit, S. M.; Fournel, M.; Bonfils, C.; Trachy-Bourget, M.-C.; Liu, J.; Yan, T. P.; Lu, A.-H.; Rahil, J.; Wang, J.; Lefebvre, S.; Li, Z.; Vaisburg, A. F.; Besterman, J. M. *J. Med. Chem.* **2007**, *50*, 5543.
16. Methot, J. L.; Chakravarty, P. K.; Chenard, M.; Close, J.; Cruz, J. C.; Dahlberg, W. K.; Fleming, J.; Hamblett, C. L.; Hamill, J. E.; Harrington, P.; Harsch, A.; Heidebrecht, R.; Hughes, B.; Jung, J.; Kenific, C. M.; Kral, A. M.; Meinke, P. T.; Middleton, R. E.; Ozerova, N.; Sloman, D. L.; Stanton, M. G.; Szewczak, A. A.; Tyagarajan, S.; Witter, D. J.; Secrist, J. P.; Miller, T. A. *Biorg. Med. Chem. Lett.* **2008**, *18*, 973.
17. The crystal structure of compound **5** in HDAC2 has been deposited in the PDB as 3MAX.
18. All compounds were characterized by $^{1}$H NMR and LC–MS, showing greater >98% purity and were consistent with reported values.
19. Schmidt, M. W.; Baldridge, K. K.; Boatz, J. A.; Elbert, S. T.; Gordon, M. S.; Jensen, J. H.; Koseki, S.; Matsunaga, N.; Nguyen, K. A.; Su, S. J.; Windus, T. L.; Dupuis, M.; Montgomery, J. A. *J. Comput. Chem.* **1993**, *14*, 1347.